

Study on the measurement accuracy of an improved cemented carbide orifice flowmeter in natural gas pipeline



Jingya Dong^{a,b}, Chengjun Jing^{c,*}, Yang Peng^d, Yang Liu^d, Hongyu Ren^e, Xianxu Liu^f

^a Institution for Disaster Management and Reconstruction, Sichuan University, Chengdu 610207, China

^b School of Engineering, Southwest Petroleum University, Nanchong 637001, China

^c College of Architecture and Environment, Sichuan University, Chengdu 610065, China

^d Gas Management Office, PetroChina Southwest Oil & Gas Field Company, Chengdu 610215, China

^e PetroChina Southwest Pipeline Company, Chengdu 610000, China

^f Chengdu Li Chuang Mold Limited Company, Chengdu 610213, China

ARTICLE INFO

Keywords:

Natural gas pipeline
Standard orifice flowmeter
Cemented carbide
Stainless steel
Discharge coefficient
Measurement accuracy

ABSTRACT

Standard orifice flowmeter has been widely used in the field of natural gas metering. However, the traditional stainless steel orifice flowmeter (TSSOF) is not resistant to wear and corrosion, especially the entrance sharpness will gradually increase. In order to improve the measurement accuracy and working life of the orifice flowmeter, the cemented carbide is embedded in the opening place of the TSSOF, thus, an improved carbide orifice flowmeter (ICOF) is manufactured. For conducting the field comparison experiment, four ICOF and four TSSOF were installed in four natural gas pipelines, respectively. The experiment results show that the variation ranges of the entrance sharpness of them are 9.863–26.438 μm and 9.192–57.329 μm , respectively; the entrance sharpness is increased with the increasing of the use time, but the change rate of the ICOF is smaller. The CFD simulation was also carried out. The simulated discharge coefficient values were compared with the calculated discharge coefficient values by the ISO empirical correlation. The results show that the accuracy of the two types of orifice flowmeter display a same decreasing trend with the increasing of the use time, and the absolute value of the relative error ranges are 0.51–2.28%, 0.13–4.25%, respectively, but the descent rate of the ICOF is smaller; the measurement accuracy of the ICOF is improved up to 2.39 times compared with the TSSOF, and it is more stable when the gas flow rate changes in the pipeline. Additionally, the effect of downstream inclination angle was studied. The result demonstrate that the measurement accuracy can be improved by 0.34%, when the downstream inclination angle is 60° at the gas flow rate of 5–15 m/s, which is superior to the commonly used inclination angle of 45°. In summary, the ICOF can be better applied to engineering practice.

1. Introduction

Even though some non-standard differential pressure type flowmeters with new structures, such as V-cone, slotted, and perforated orifices, show higher accuracy and better adaptability in some measuring conditions, the standard orifice plate remains the instrument of choice for many flow metering applications due to its simple design, high reliability and low cost. It is by far the most widely used flowmeter in industrial service, accounting for over 40% of the market including oil and gas, chemical, nuclear, power engineering, etc [1–5]. Its measuring mechanism is based on a firm relationship between the pressure drop and the volumetric flow rate. Different application range of differential pressure type flowmeters have captured enough attention in the past decades, and the increasing demands for more accurate flow

measurements have made the study of pulsating flow effects crucial for the further development of flowmeter [6,7]. In the recent work, a combination of experimental measurements and computational fluid dynamics (CFD) were utilized to characterize the behavior of various flowmeters. In particular, the CFD method for predicting the discharge coefficient value was verified through comparison with laboratory data [8–10].

He et al. [11] proposed a dimensionless parameter to correct the discharge coefficient when the V-cone orifice was used to measure wet gas flow rate. The results demonstrate that the relative error of the gas mass flow rate is within $\pm 5\%$ at the velocity range from 4.87 to 25.26 m/s, and the relative error of the liquid mass flow rate is within $\pm 5\%$ at the velocity range from 0 to 0.38 m/s. Singh et al. [12] studied the effect of upstream disturbance on discharge coefficient of

* Corresponding author.

E-mail address: chengjunjing@126.com (C. Jing).

the V-cone flowmeter. It shows that the value of the discharge coefficient is not affected by the upstream disturbance if the disturbance is placed at a distance of $10D$ or more. However, the variation of discharge coefficient is up to 6% when the distance is less than $5D$. McIver and Peter [13] analyzed the stability on discharge coefficient of the V-cone orifice, and the results show that the discharge coefficient variation is $\pm 2\%$ over a wide range of Reynolds number. Although the V-cone orifice is accurate and less sensitive to Reynolds number, it is not widely used due to its complexity structure.

Recently, systematic investigation on the discharge coefficient have regard to slotted orifice [14]. The slotted orifice has found to be substantially less sensitive to upstream flow conditions, and it is also a better choice for two phase flow metering [15,16]. Hua and Geng [17] predicted the gas mass flow rate with an slotted orifice. The result shows that the relative errors were within $\pm 6\%$, which is accepted for many two phase flow application. From the literature available, the slotted orifice has a simpler structure than the V-cone orifice, but it is still not widely used, because it is more suitable for measuring the wet gas.

Structurally, a perforated orifice can be treated as a combination of a standard orifice and a slotted orifice, which can avoid some disadvantages of the V-cone orifice and the slotted orifice to some extent. Manshoor et al. [18] did a research on the relationship between the orifice shape and the discharge coefficient by the experiment method and the CFD simulation. The result shows that an optimal shape can reduce the installation length. Malavasi et al. [19] tested several perforated plates with different geometrical characteristics, and the relative error of the pressure loss coefficient was found to be low. Ma et al. [20] reported some experimental results on pressure drop and discharge coefficient of a perforated orifice. The results show that a perforated orifice has characteristic of anti-disturbance. Huang et al. [21] tested a perforated orifice, and the experimental results present that the perforated orifice has a low critical Reynolds number and a strong anti-disturbance ability. Singh and Tharakan [22] used the CFD method to simulate the perforated orifice with different shapes. The results demonstrate that a perforated orifice has low pressure loss. Despite the advantages of the perforated orifice, the structure of it is still crucial to the performance as a flowmeter. The perforated orifice with different structures may lead to difference when it is used to measure gas flow. According to the literature, the experiment and CFD simulation approaches are only preliminary attempt, and little experimental data can be obtained.

According to the published literatures, nowadays researches about the measurement accuracy are focus on the change of flowmeter structure, which will increase the complexity of the flowmeter structure and not easy to use them in actual natural gas pipelines [23]. The standard orifice flowmeter has a long history and an extensive using range. In Chinese oil and gas industry, the use of standard orifice flowmeter for measurement accounted for about 95% of the total flowmeter [24]. The traditional stainless steel orifice flowmeter (TSSOF) usually have the shortcomings of low hardness, easy corrosive, poor wear resistance, weak impact performance and not easy to deeply process the downstream inclination angle. In particular, for the unclean fluid containing fine particles and corrosive fluids with high acid components such as H_2S and CO_2 , the upstream entrance sharpness of the orifice plate will gradually decrease. Aly et al. [25] did a experimental study on the pressure drop after fractal-shaped orifices in a turbulent flow pipe. In reality, an orifice plate will have different abrasion forms as fractal-shaped orifice. However, we simplified all cased to a circular arc form in order to build the model easily in this paper, as shown in Fig. 1. Structure change and the dependence of the pressure loss coefficient on the flow rate through the flow restrictors [26] will result in a significant reduction in accuracy and servicing life in accordance with Chinese standard, GB/T 21446-2008 [27], and ISO 5167 [28] during a short period of time. Therefore, it is necessary to further improve the TSSOF measurement accuracy from the perspective

of introducing a new sort of material.

Based on the above reason, a cemented carbide is embedded in the opening place of a standard stainless steel orifice flowmeter. The cemented carbide is mainly made of wolfram carbide (WC) whose hardness is similar to the diamond, and it insoluble in water, hydrochloric acid and sulfuric acid. Thereby, an improved Carbide Orifice Flowmeter (ICOF) is manufactured [29]. The comparison for the structures of the two types of standard orifice flowmeters are shown in Fig. 2.

In order to verify the measurement accuracy of the ICOF, the field test was firstly carried out. Four ICOF and four TSSOF were installed in four different natural gas pipelines, namely one ICOF and one TSSOF were installed in a same pipeline. During one year experiment period, the two types of orifice flowmeters installed in the pipeline were taken out at regular intervals to detect the change of the entrance sharpness, then the test results were analyzed and compared. Afterwards, the CFD software FLUENT was used to simulate the operation conditions of the two types of orifice flowmeters. To study the difference in measurement accuracy, the discharge coefficient values of the two types of orifice flowmeter were compared with the calculated values by the ISO empirical correlation. Finally, the suitability of the cemented carbide orifice flowmeter was evaluated.

2. Theoretical analyses

The measurement accuracy of the standard orifice flowmeter is characterized by the deviation between the discharge coefficient calculated from the actual measurement and the discharge coefficient calculated from the empirical equation given by the ISO standard. The two types of orifice flowmeters were installed in the same pipeline, which was easy to compare the measurement accuracy. Fig. 3 displays the installation of the two types of orifice flowmeter in the natural gas pipeline of the field. According to the actual situation of the field, the upstream diameter of the pipeline D is 104 mm, the distance between the two types of orifice flowmeter is larger than that of ISO 5167, which is 0.52 m, and the downstream straight pipeline is larger than $10D$, namely 1.04 m. According to ISO 5167 and GB/T 21446-2008, one orifice plate should be installed with enough upstream and downstream spaces, and a pair of orifice plates should surely be separated by much longer distances. In real situation, we separated the two plates by at least 2.75 m, which is more than 26 times of the upstream diameter. The measurement principle is that if the fluid passes through the orifice plate, due to the decreasing of the flow area, the pressure energy is partially converted into kinetic energy, which causes a significant pressure difference in front and back of the orifice plate. Thereby, the fluid flow can be measured by monitoring the value of pressure. The way of taking pressure is the "D-D/2" method.

For a differential pressure device, using the basic principle of conservation of mass and energy balance across the throttling element, the performance equation for the standard orifice can be obtained by the follows:

$$q_v = \frac{C'\varepsilon}{\sqrt{1-\beta^4}} \cdot \frac{\pi d^2}{4} \cdot \sqrt{2\Delta p/\rho} \quad (1)$$

where, q_v is the actual volume flow, m^3/s ; C' is the discharge coefficient; β is the diameter ratio; d is the hole diameter, m; Δp is the pressure difference before and after the orifice, Pa; ρ is density of the fluid, kg/m^3 . The ε is an expansibility factor being unity for an incompressible fluid. The diameter ratio, β , is determined by the orifice diameter of primary device under working conditions, d , to the upstream pipeline diameter, D :

$$\beta = \frac{d}{D} \quad (2)$$

The calculation method of C' can be derived from the formula (1) as follows:

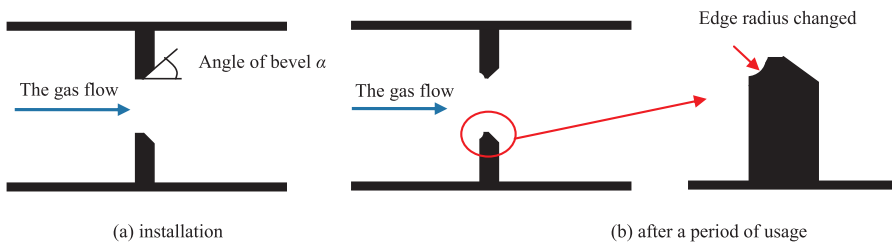


Fig. 1. Sketch of the orifice entrance sharpness change with time (a) installation (b) after a period of usage.



Fig. 2. Two kinds of orifice flowmeters: the TSSOF and the ICOF.

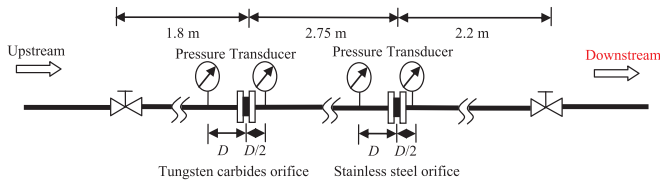


Fig. 3. The installation of the two types of orifice flowmeter in the natural gas pipeline.

$$C' = \frac{q_v \sqrt{1 - \beta^4}}{\frac{\pi d^2}{4} \varepsilon \sqrt{2 \Delta p / \rho}} \quad (3)$$

According to the correlation (3), under the premise of knowing the fluid flow q_v , the discharge coefficient C' can be obtained by solving the pressure difference before and after the orifice plate, and the pressure difference can be obtained by the pressure sensor installed on the pipeline. In practical engineering application, the orifice flowmeter measures the flow rate q_v of the fluid, at this time, C' needs to be regarded as a known condition. For the standard orifice flowmeter, at the time of leaving the factory, it is assumed that the C' is exactly equal to the discharge coefficient C specified in ISO 5167, and it is calculated by follows:

$$C = 0.5961 + 0.0261\beta^2 - 0.216\beta^8 + 0.000521 \left(\frac{10^6 \beta}{Re_D} \right)^{0.7} + (0.0188 + 0.0063A)\beta^{3.5} \left(\frac{10^6}{Re_D} \right)^{0.3} + (0.043 + 0.080e^{-10L_1} - 0.123e^{-7L_2}) (1 - 0.11A) \frac{\beta^4}{1 - \beta^4} - 0.031(M - 0.8M^{1.1})\beta^{1.3} \quad (4)$$

where, L_1 is the quotient of the distance of the upstream tapping from the upstream face of the plate and the pipe diameter, L_2 is the quotient of the distance of the downstream tapping from the downstream face of the plate and the pipe diameter, Re_D is the Reynolds number calculated with respect to D :

$$Re_D = \frac{\bar{u} D \rho}{\mu} \quad (5)$$

where, \bar{u} is the mean axial velocity of the fluid in the pipe; μ is the dynamic viscosity.

In Eq. (4), the factor A and M are calculated as follows:

$$A = \left(\frac{19000\beta}{Re_D} \right)^{0.8} \quad (6)$$

$$M = \frac{2L_2}{1 - \beta} \quad (7)$$

In accordance with the provisions of ISO 5167, the upstream edge of the orifice plate should be 90° , smooth with no burr, and the upstream end of the entrance sharpness $r \leq 0.0004 d$. However, in practical engineering applications, the size of the orifice plate itself will inevitably be worn and changed, so that the actual discharge coefficient value C' will gradually deviate from the design value C , thereby, the measurement accuracy of the flowmeter will reduce. Thus, the deviation value of the discharge coefficient can be used to predict the measurement accuracy change for different material standard orifice flowmeters.

3. Field experiment

The two types of orifice flowmeters were installed in the actual pipeline to use about 1 year, during this period, the orifice plates were taken out for the detection of the entrance sharpness every three months, and then the data of the two types of orifice flowmeters were obtained.

In this study, we adopt the portable orifice automatic measuring instrument (HXJ – 150 A) which is widely used in oil and natural gas extraction in China. It is a special instrument to detect gas metering device, which applies the optical imaging, grating displacement sensor and piezoelectric crystal sensor principle to measure the thickness, surface roughness, entrance sharpness and other parameters of the orifice flowmeter. The instrument is composed of an optical system, a mechanical system, a control system and a notebook computer, as shown in Fig. 4.

A special measuring microscope was used to measure the entrance sharpness of the orifice flowmeter. The test principle is that the optical imaging method is used to image the maximum wear point at the entrance edge of the orifice plate, then four measurements are carried out with the micrometer eyepiece, and the measurement results are entered into the software on the laptop for automatic calculation. The measurement uncertainty of the measuring microscope is $4 \mu\text{m}$. The results in this work are the average of four measurements, and since the output data of the computer has many decimal digits, the study reserves 3 decimal places.



Fig. 4. The HXJ – 150 A portable orifice automatic measuring instrument.

After about one year, the entrance sharpness of the ICOF installed in the 1# and 2# pipelines increased by 2.214 μm and 3.778 μm , respectively, while the TSSOF entrance sharpness increased by 14.196 μm and 16.103 μm , respectively. Thus, with the increasing of use time, the ICOF have a better performance in wear resistant property than that of the TSSOF. For the ICOF installed in 3# pipeline, its entrance sharpness was 22.804 μm at the first test, while the entrance sharpness of the TSSOF was 41.896 μm . Therefore, the entrance sharpness of the TSSOF is 1.84 times than that of the ICOF. However, for the fourth test at 9/13/2015, the entrance sharpness of the ICOF was increased to 26.438 μm , and the entrance sharpness of the TSSOF was 57.329 μm . Thus, the entrance sharpness of the TSSOF is 2.16 times than that of the ICOF. For the 4# pipeline, the initial entrance sharpness of the ICOF was 13.612 μm , while the entrance sharpness of the TSSOF was 26.345 μm , and the entrance sharpness of the TSSOF is 1.94 times than that of the ICOF. In the fourth test at 9/13/2015, the entrance sharpness of the ICOF increased to 15.617 μm , and the entrance sharpness of the TSSOF was 34.986 μm . Thus, the entrance sharpness of the TSSOF is 2.24 times than that of the ICOF. Therefore, with the increasing of use time, the ICOF have a better performance in wear resistant property than that of the TSSOF.

Fig. 5(a) to (d) show the comparison results of the entrance sharpness increasing rate (relative to the firstly detection time) of the two types of orifice flowmeters in the four pipelines at different detection times. It can be seen that with the increasing of use time, the entrance sharpness of the two types of orifice flowmeters installed in different pipelines showed a same gradual increasing trend, but the increasing rate of the ICOF is smaller, which reflecting the more excellent wear resistance.

4. Model development

Although it is directly and clearly observed that the ICOF is more wear resistance by field experiment, the influence of the entrance sharpness change on the natural gas flow measurement accuracy still needs to be further studied. In order to obtain the measurement accuracy of the two types of orifice flowmeters under different entrance sharpness, the CFD software FLUENT was used to establish the simulation model. Through analyzing the deviation of the discharge coefficient value between the numerical simulation and the empirical formula recommended by the ISO standard, the difference in measurement accuracy of the two types of orifice flowmeters can be determined.

4.1. Geometry details

The two types of orifice flowmeters used in the field experiment have the same geometrical shape: the orifice plate thickness, E , is 4 mm, the throttles thickness, e , is 1.5 mm, upstream pipe diameter, D , is 104 mm, the orifice diameter, d , is 50 mm, the aperture ratio, β , is 0.48, and the geometric model used in the CFD modeling is shown in Fig. 6. Under the impact of flow, different degrees and different forms of abrasion will be presented. In this study, we simplified all cases to a circular arc form in order to easily build the geometry model.

4.2. Computational mesh

Since the standard orifice flowmeter can be simplified as an axial symmetry model, it can be simulated by establishing the two-

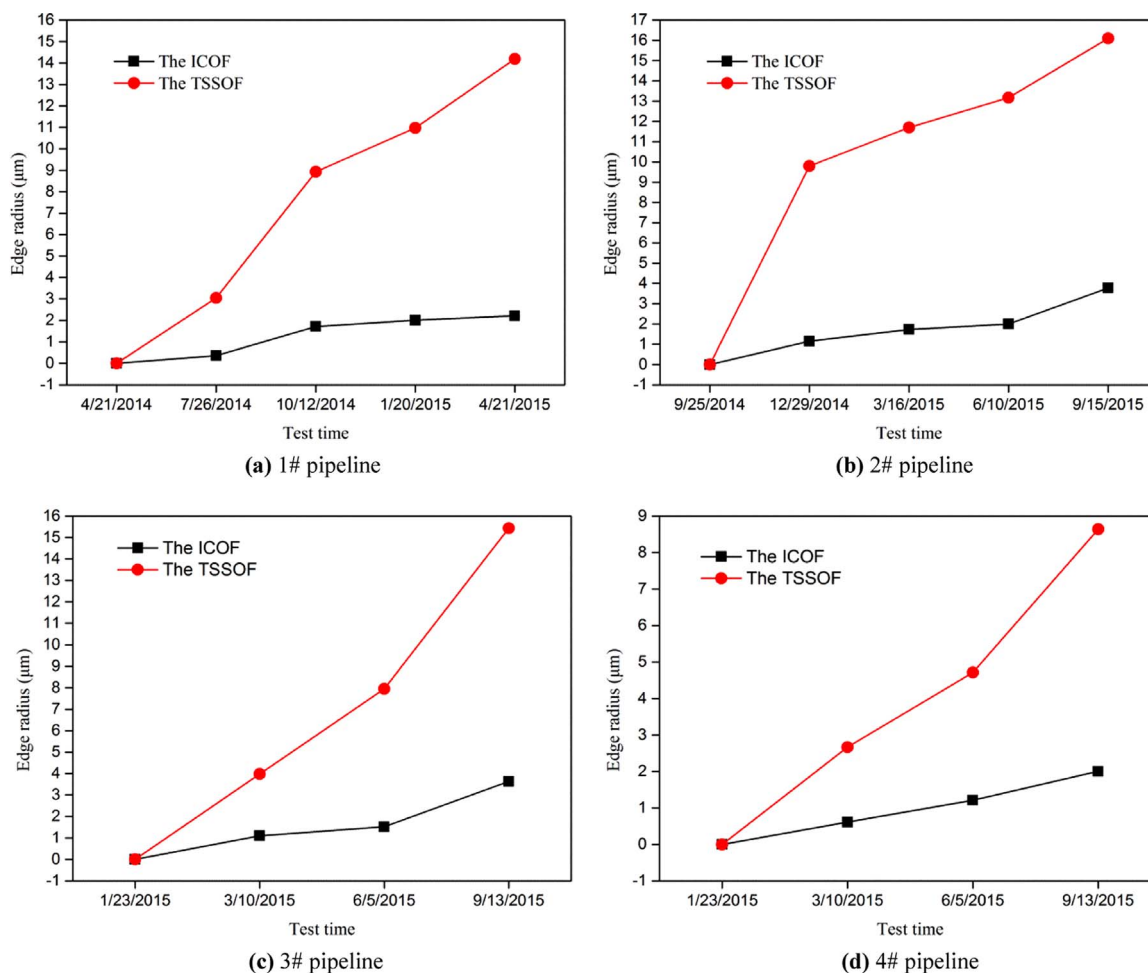


Fig. 5. Comparison of the entrance sharpness increasing rate of the two types of orifice flowmeters installed in different pipelines. (a) 1# pipeline (b) 2# pipeline (c) 3# pipeline (d) 4# pipeline.

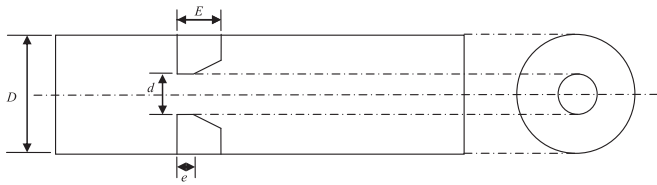


Fig. 6. The geometry model of the orifice flowmeter.

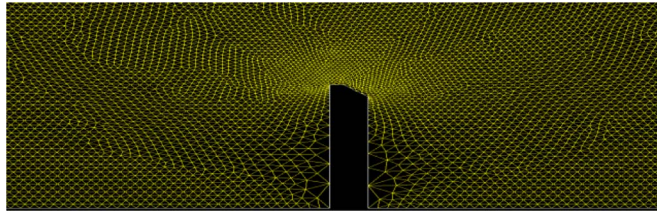


Fig. 7. The two-dimensional geometric model and the grid partitioning result of the orifice flowmeter.

Table 1

The comparison results of the discharge coefficient between the numerical simulation and ISO empirical correlation at different flow rates.

Velocity (m/s)	The value of discharge coefficient		ARE (%)
	ISO correlation, C_{ISO}	Numerical simulation, C_{cal}	
1	0.6109	0.6120	0.18%
3	0.6054	0.6081	0.45%
5	0.6040	0.6060	0.33%
8	0.6030	0.6041	0.18%
10	0.6027	0.6040	0.22%
15	0.6021	0.6038	0.28%
20	0.6019	0.6033	0.23%

dimensional model. Sheikholeslami and Barry [30,31] used the axial symmetry model in the FLUENT software to simulate the changing situation of the orifice flowmeter with the Reynolds number, diameter ratio, pipe surface roughness, upstream vortex, upstream and downstream flow boundary conditions. They obtained that the discharge coefficient value was within 2% compared with the empirical correlation. Araoye et al. [32] also used the FLUENT software to build a two-dimensional model of the orifice flowmeter, and the grid independence of 57310 grids, 129,858 grids and 230,500 grids, respectively. The result indicates that the computation error was within 2%. Li et al. [33] established a two-dimensional axial symmetry model of the standard

Table 2

The velocity, Reynolds number and the discharge coefficient calculated by the ISO correlation.

Velocity (m/s)	Reynolds number	The discharge coefficient, C_{ISO}
5	31,951	0.6040
8	51,121	0.6030
10	63,902	0.6027
12	76,683	0.6021
15	95,853	0.6019

orifice by using the FLUENT software, and the velocity and pressure fields were calculated by dividing the triangular mesh.

Although the structured mesh is more widely used in the numerical simulation of orifice plate, we focus on the edge radius change, and it is a very small change which makes the orifice plate have a more complicated structure. Therefore, the unstructured mesh was introduced in this work, and we have used local grid refinement method to make the simulation results more reliable. This study adopted the FLUENT software to build a two-dimensional model of the orifice flowmeter. The triangular grid was utilized to divide the face grid, and the grids at the opening place of the orifice plate was encrypted, as shown in Fig. 7. Owing to the fact that there will be vortexing or stagnant flow on the downstream of orifice plate, we made a grid independence verification. The results show that there are no significant differences between the grids number of 192,694 and 278,393 at the inlet flow rate of 8 m/s. Therefore, a finer mesh division has little effect, so the selected meshing method can be applied for the simulation.

4.3. Governing equations

The governing equations for the gas flow are given as follows:

(1) Continuity equation

$$\frac{\partial \rho}{\partial t} + \nabla \cdot (\rho \vec{u}) = 0 \tag{8}$$

(2) Momentum equation

$$\frac{\partial}{\partial t} (\rho \vec{u}) + \nabla \cdot (\rho \vec{u} \vec{u}) = -\nabla p + \nabla \cdot \tau \tag{9}$$

(3) Energy balance

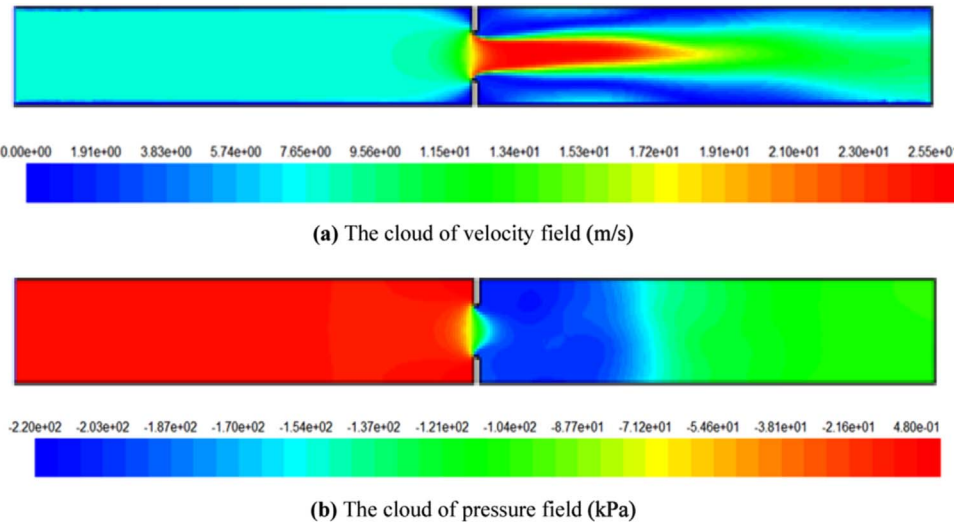


Fig. 8. The simulation results of the standard orifice flowmeter by using the FLUENT software. (a) The cloud of velocity field (m/s) (b) The cloud of pressure field (kPa).

Table 3
The results of the discharge coefficient for the ICOF and the TSSOF at 5–15 m/s.

Pipeline number	Test time	Flow velocity (m/s)									
		5		8		10		12		15	
		The ICOF, C_{cal1}	The TSSOF, C_{cal2}	The ICOF, C_{cal1}	The TSSOF, C_{cal2}	The ICOF, C_{cal1}	The TSSOF, C_{cal2}	The ICOF, C_{cal1}	The TSSOF, C_{cal2}	The ICOF, C_{cal1}	The TSSOF, C_{cal2}
1#	4/21/2014	0.6071	0.6106	0.6067	0.6093	0.6063	0.6087	0.6061	0.6075	0.6059	0.6073
	7/26/2014	0.6095	0.6121	0.6084	0.6103	0.6082	0.6102	0.6073	0.6094	0.6071	0.6094
	10/12/2014	0.6109	0.6156	0.6095	0.6143	0.6091	0.6128	0.6089	0.6122	0.6081	0.6108
	1/20/2015	0.6135	0.6189	0.6106	0.6167	0.6099	0.6146	0.6097	0.6137	0.6094	0.6127
2#	4/21/2015	0.6178	0.6214	0.6117	0.6195	0.6116	0.6162	0.6107	0.6152	0.6106	0.6150
	9/25/2014	0.6092	0.6062	0.6090	0.6055	0.6089	0.6046	0.6080	0.6046	0.6075	0.6029
	12/29/2014	0.6096	0.6163	0.6092	0.6118	0.6089	0.6115	0.6085	0.6113	0.6081	0.6097
	3/16/2015	0.6097	0.6157	0.6093	0.6145	0.6092	0.6132	0.6091	0.6125	0.6089	0.6108
3#	6/10/2015	0.6097	0.6205	0.6105	0.6186	0.6096	0.6157	0.6094	0.6155	0.6092	0.6135
	9/15/2015	0.6107	0.6256	0.6102	0.6222	0.6098	0.6183	0.6096	0.6166	0.6095	0.6153
	1/23/2015	0.6112	0.6236	0.6110	0.6231	0.6106	0.6217	0.6102	0.6205	0.6099	0.6179
	3/10/2015	0.6165	0.6264	0.6143	0.6259	0.6131	0.6253	0.6131	0.6236	0.6128	0.6205
4#	6/5/2015	0.6169	0.629	0.6159	0.6288	0.6138	0.6271	0.6136	0.6254	0.6137	0.6211
	9/13/2015	0.6174	0.6297	0.6172	0.6295	0.6147	0.6280	0.6145	0.6267	0.6143	0.6240
	1/23/2015	0.6119	0.6178	0.6100	0.6170	0.6094	0.6162	0.6088	0.6152	0.6081	0.6135
	3/10/2015	0.6137	0.6218	0.6103	0.6240	0.6102	0.6180	0.6094	0.6170	0.6086	0.6150
	6/5/2015	0.6152	0.6256	0.6129	0.6215	0.6128	0.6215	0.6111	0.6200	0.6102	0.6177
	9/13/2015	0.6152	0.6291	0.6143	0.6268	0.6136	0.6233	0.6128	0.6218	0.6110	0.6207

$$\frac{\partial}{\partial t}(\rho E) + \nabla \cdot (\vec{u}(\rho E + p)) = 0$$

$$E = h - \frac{p}{\rho} + \frac{\mu^2}{2} \tag{10}$$

where, ρ is the density, u is the velocity, p is the pressure, τ is the viscous stress tensor, h is the enthalpy. Comparing with the standard κ - ϵ model, the RNG κ - ϵ model is more accurate when the streamline bending degree is larger and strain rate is higher. Therefore, the RNG κ - ϵ model was chosen in this study.

4.4. Boundary conditions

In China, some large-caliber long distance pipelines are used for transmission natural gas through high pressure. However, for the medium and low pressure city gas pipelines or the small diameter natural gas pipelines, the operating pressures are usually low (< 0.4 MPa). Therefore, the pressure similar to ambient pressure (0.1 MPa) was selected for calculation. The improved orifice flowmeter developed in this study has the characteristics of wear resistance and corrosion resistance. It is mainly applicable to transport natural gas containing solid particles such as fine sand, and acidic gases such as H₂S and CO₂. Hence, the gas flow rate caused by high pressure can have a certain effect on the life of orifice, but it is not the main one.

The boundary conditions of the simulation were set as follows: the inlet boundary condition adopted the natural gas flow rate, regardless of the pressure change of the operating condition; the export boundary condition adopted the natural gas outlet flow; the natural gas pipe wall condition used the actual test data, and the no-slip condition was considered between the wall and the fluid. In order to verify the accuracy of the model, the methane at room temperature was selected as a fluid medium, and the values of its density, viscosity and other parameters were determined by the software itself database.

4.5. Model verification

By obtaining the average pressure values of the D and $D/2$ section of the orifice flowmeter, the discharge coefficients (C_{cal}) at the speed of 1 m/s, 3 m/s, 5 m/s, 8 m/s, 10 m/s, 15 m/s and 20 m/s were determined, which were utilized to compare with the calculation results of ISO empirical correlation (C_{ISO}) under the same conditions. The results are listed in Table 1. The Absolute value of the Relative Error (ARE) is calculated as following:

$$ARE = \left| \frac{C_{cal} - C_{ISO}}{C_{ISO}} \right| \times 100\% \tag{11}$$

From Table 1, it can be seen that the deviation of the C_{cal} and the C_{ISO} , are less than 0.5% at the flow rate range of 1–20 m/s. Therefore, the simulation model established in this work by adopting the FLUENT software can be used for determining the discharge coefficient of the orifice flowmeter. The simulation results of velocity field and the pressure field at the flow rate of 8 m/s for the standard orifice flowmeter are shown in Fig. 8.

5. Results and discussion

5.1. The effect of entrance sharpness change

According to the current operation of the actual natural gas pipeline, the simulation model for the ICOF and the TSSOF were established to calculate the discharge coefficient. According to Chinese Gas Planning and Design Handbook [34], natural gas velocity must lower than 30 m/s. The velocities of 5–15 m/s as the "economic velocity" when the pipeline diameter is less than 150 mm are recommended. Hence, we utilized the velocity range from 5 to 15 m/s to build the CFD model. The range of natural gas flow velocity, Reynolds number and the result calculated by

Table 4
The comparison results of the ARE for the two types of orifice flowmeters at 5–15 m/s.

Pipeline number	Test time	Flow velocity (m/s)														
		5			8			10			12			15		
		The ICOF ARE (%)	The TSSOF ARE (%)	The ICOF ARE (%)	The TSSOF ARE (%)	The ICOF ARE (%)	The TSSOF ARE (%)	The ICOF ARE (%)	The TSSOF ARE (%)	The ICOF ARE (%)	The TSSOF ARE (%)	The ICOF ARE (%)	The TSSOF ARE (%)			
1#	4/21/2014	0.51	1.09	0.61	1.05	0.61	1.00	0.62	0.84	0.63	0.86	0.86	1.20			
	7/26/2014	0.91	1.34	0.89	1.21	0.93	1.26	0.82	1.16	0.83	1.20	1.20	1.44			
	10/12/2014	1.14	1.92	1.07	1.87	1.06	1.68	1.08	1.63	1.00	1.44	1.44	1.74			
	1/20/2015	1.57	2.47	1.25	2.27	1.20	1.99	1.21	1.87	1.20	1.74	1.74	2.13			
2#	4/21/2015	2.28	2.88	1.45	2.73	1.48	2.24	1.38	2.12	1.36	2.13	2.13	2.13			
	9/25/2014	0.86	0.36	0.99	0.41	1.04	0.33	0.92	0.26	0.89	0.13	0.13	0.13			
	12/29/2014	0.93	2.04	1.03	1.46	1.04	1.46	1.02	1.48	1.00	1.26	1.26	1.26			
	3/16/2015	0.94	1.94	1.05	1.90	1.08	1.74	1.11	1.68	1.13	1.43	1.43	1.43			
3#	6/10/2015	0.94	2.73	1.19	2.59	1.15	2.17	1.16	2.16	1.17	1.88	1.88	1.88			
	9/15/2015	1.11	3.58	1.24	3.18	1.18	2.60	1.19	2.36	1.22	2.19	2.19	2.19			
	1/23/2015	1.19	3.25	1.32	3.33	1.32	3.16	1.29	3.00	1.29	2.61	2.61	2.61			
	3/10/2015	2.07	3.71	1.87	3.80	1.74	3.76	1.77	3.51	1.77	3.04	3.04	3.04			
4#	6/5/2015	2.14	4.14	2.13	4.28	1.84	4.06	1.86	3.82	1.91	3.15	3.15	3.15			
	9/13/2015	2.22	4.25	2.36	4.39	2.00	4.21	2.00	4.03	2.02	3.62	3.62	3.62			
	1/23/2015	1.31	2.28	1.16	2.32	1.12	2.25	1.07	2.12	1.00	1.89	1.89	1.89			
	3/10/2015	1.61	2.95	1.20	2.55	1.26	2.54	1.15	2.42	1.06	2.13	2.13	2.13			
6/5/2015	1.85	3.58	1.65	3.48	1.68	3.12	1.44	2.92	1.34	2.59	2.59	2.59				
	9/13/2015	1.85	4.16	1.87	3.95	1.82	3.42	1.73	3.22	1.47	3.09%	3.09%				

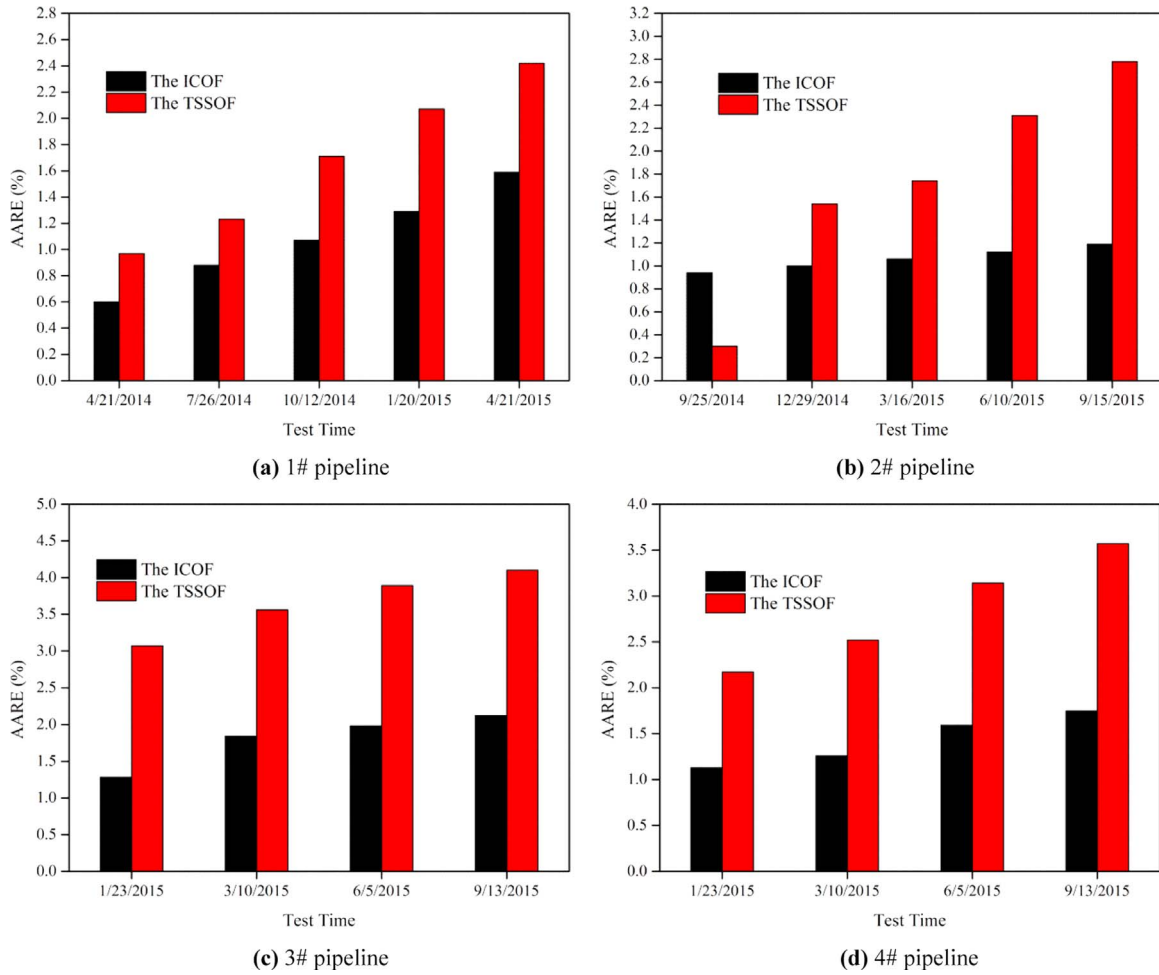


Fig. 9. The comparison results of the AARE for the two kinds of orifice flowmeters. (a) 1# pipeline (b) 2# pipeline (c) 3# pipeline (d) 4# pipeline.

the ISO correlation are shown in Table 2. The results of the discharge coefficient for the ICOF (C_{cal1}) and the TSSOF (C_{cal2}) installed in the four pipelines are listed in Table 3; the comparison results of the ARE for the two types of orifice flowmeters at 5–15 m/s are listed in Table 4.

From Tables 2–4, it can be seen that the discharge coefficients of the ICOF, C_{cal1} , are closer to the calculation value by the ISO correlation, C_{ISO} , and the ARE is smaller than that of the TSSOF. During the field experiment period, when the natural gas flow rate range is 5–15 m/s, the ARE of the ICOF installed in the 1# pipeline is in the range of 0.51–2.28%, while the ARE range of the TSSOF is 0.84–2.88%; the ARE of the ICOF installed in the 2# pipeline is in the range of 0.86–1.24%, while the ARE range of the TSSOF is 0.13–3.58%; the ARE of the ICOF installed in the 3# pipeline is in the range of 1.19–2.36%, while the ARE range of the TSSOF is 2.61% to 4.39%; the ARE range of the ICOF installed in the 4# pipeline is 1.00–1.87%, while the ARE range of the TSSOF is 1.89–4.16%. Therefore, it can be concluded that the ARE range of the ICOF is smaller and the ARE value is less than that of the TSSOF.

According to Table 3, the average absolute value of the relative error (AARE) of the discharge coefficient for the two kinds of orifice flowmeters in the flow velocity range of 5–15 m/s at different test time can be computed by the following correlations:

$$AARE = \frac{1}{N} \sum_i \left| \frac{C_{cali} - C_{ISOi}}{C_{ISOi}} \right| \times 100\% \quad (12)$$

The comparison results of the AARE for the two kinds of orifice flowmeters are drawn in Fig. 9 (a) to (d).

It can be seen from Fig. 9(a) to (d) that the AARE of the two types of

orifice flowmeters are increased with the increasing of use time, but the AARE increasing rate of the TSSOF is higher; when the natural gas flow rate range is 5–15 m/s, the AARE range of the ICOF is 0.60–2.12%, while the AARE range of the TSSOF is 0.30–4.10%, so the change range of the ICOF is smaller; the AARE of the ICOF can be increased up to 1.98% compared with the AARE of the TSSOF; when the flow rate range is 5–15 m/s, the measurement accuracy of the AARE is significantly less than that of the TSSOF, namely the measurement accuracy of the ICOF is higher.

The comparison results of the AARE for the two types of orifice flowmeters at 5–15 m/s are displayed in Fig. 10(a) to (d).

It can be seen from Fig. 10(a) to (d) that the AARE of the ICOF is less than 2%, while the AARE of the TSSOF reached to 3.95% in the one year experiment period; the AARE of the ICOF is smaller at the same flow rate during the one year experiment period, therefore, the measurement accuracy of it is higher; with the gas flow rate increasing from 5 to 15 m/s, the AARE of the TSSOF showed a downward trend; the results indicate that the greater of the natural gas flow rate is the higher of the measurement accuracy.

In order to study the variation range of the measurement accuracy for the two kinds of orifice flowmeters, the standard deviation (SD) of the calculation results of the discharge coefficient was determined. The SD of the two types of orifice flowmeters are shown in Fig. 11. The SD is calculated as follows:

$$SD = \sqrt{\frac{\sum_{i=1}^n (s_i - \bar{s})^2}{n}} \quad (13)$$

where, SD is standard deviation; s_i is measurement value; \bar{s} is arithmetic

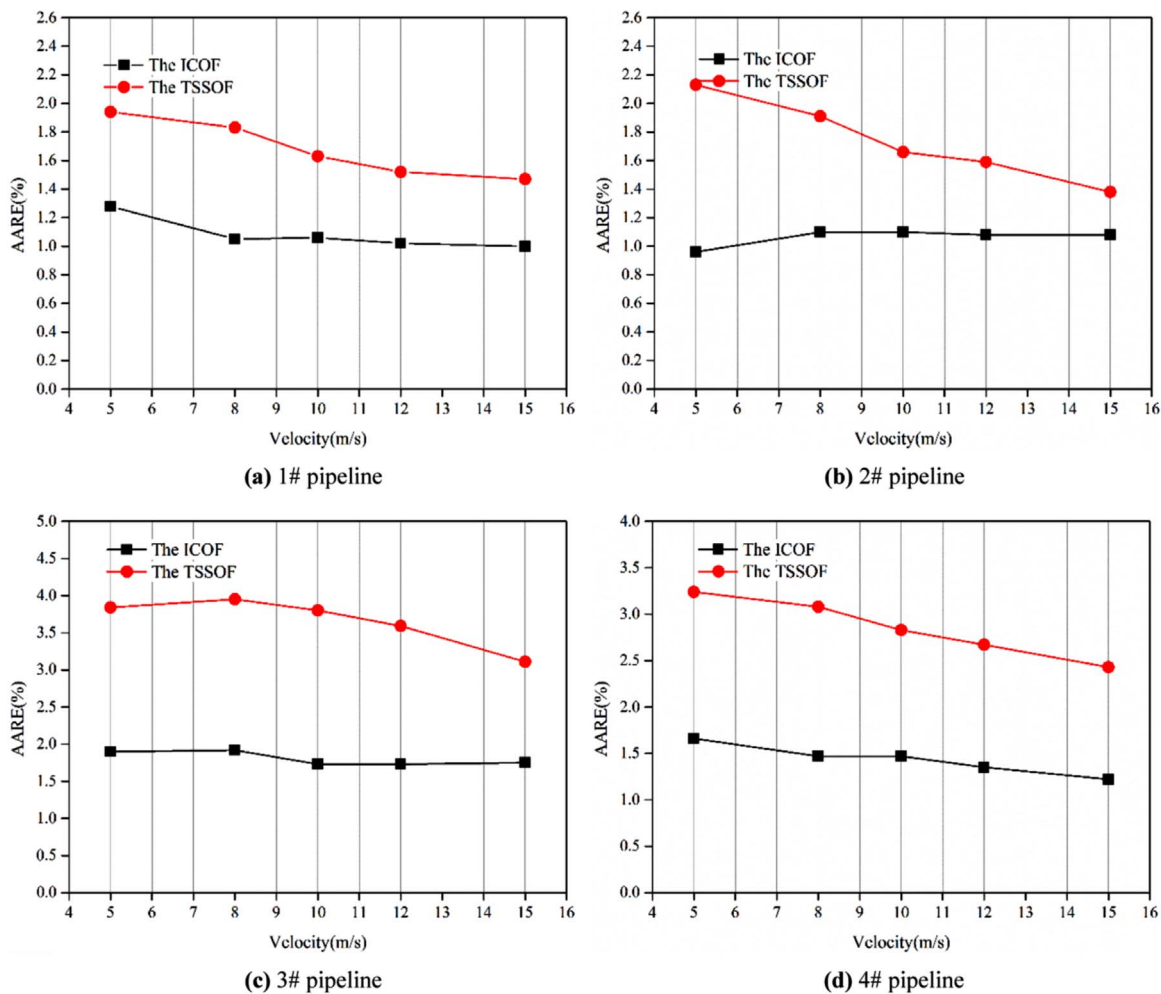


Fig. 10. The comparison results of the AARE for the two types of orifice flowmeters at 5–15 m/s. (a) 1# pipeline (b) 2# pipeline (c) 3# pipeline (d) 4# pipeline.

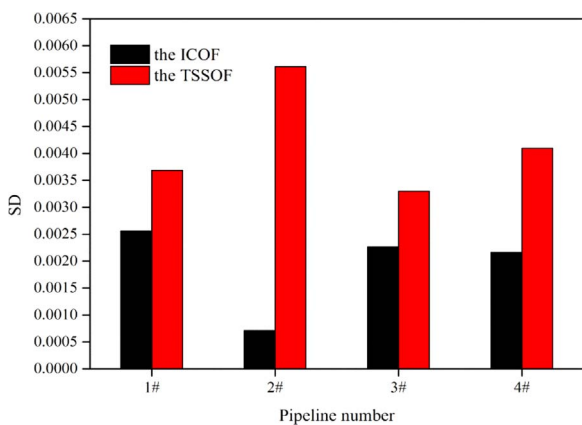


Fig. 11. The standard deviation of the two types of orifice flowmeter.

mean value; n is test times.

As it can be clearly seen from Fig. 11 that the SD of the ICOF is less than that of the TSSOF, so the measurement accuracy of the ICOF is more stable and reliable.

5.2. The effect of downstream inclination angle change

According to Chinese standard GB/T 21446-2008, the bevel angle is recommended to be $45^\circ \pm 15^\circ$. However, when the low-hardness stainless steel is used, the excessive machining angle can cause thinner

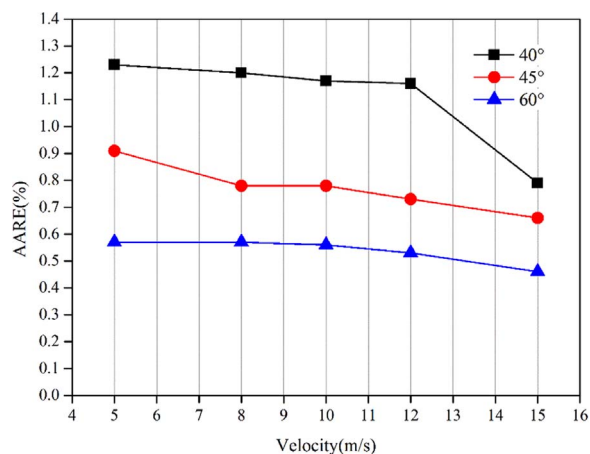


Fig. 12. The comparison results of the ARE for the discharge coefficient at 5–15 m/s.

thickness at the entrance place. It is more likely to fail, when the gas flow is constantly impacted on the plate entrance place. While the cemented carbide can overcome the shortcoming, and also improve the measurement accuracy according to the research results.

Some researchers studied in the effect of orifice plate geometry upon discharge coefficient and the results showed that having a 30° angle to the bore, or having a 60° angle to the bore made a negligible difference from having a 45° angle [35–38]. Dong et al. [39] studied the measurement accuracy of the ICOF when the downstream inclination

angle were 40°, 45° and 60°, respectively, at the natural gas flow rate of 8 m/s. The measurement accuracy error was 0.57% when the inclination angle was 60°, while the error of the commonly used 45° angle was 0.78%, and the error of the 40° angle was 1.2%. The results indicate that when the downstream inclination angle set as 60°, the measurement accuracy is higher. Therefore, the downstream end face of the ICOF which has high strength and high abrasion resistance can be machined to 60°. However, since the speed of the previous study is single, it can not be determined whether the ICOF has an inclination angle of 60° will be applied to other flow rates.

According to *Chinese Gas Plan and Design Handbook*, the natural gas velocity must lower than 30 m/s. Besides, a velocity range named "economic velocity" which is 5–15 m/s when the pipeline diameter is less than 150 mm is recommended for actual natural gas pipelines in China. Therefore, a relatively narrow range of Reynolds number (32,000 – 95,000) was chosen to study the effect of different bevel angle on measurement accuracy. In this work, the downstream inclination angle values were taken as 40°, 45° and 60°; the gas flow rate were 5 m/s, 8 m/s, 10 m/s, 12 m/s and 15 m/s. The FLUENT software was used to simulate, thus the values of the discharge coefficient C_{cal} were obtained. Then the results were compared with the C_{ISO} . The comparison results of the ARE for the discharge coefficient at the same flow rate and different inclination angles are shown in Fig. 12.

From the trend of AARE% for the discharge coefficient in Fig. 12, it can be concluded that the error of the discharge coefficient tends to decrease gradually with the gas flow rate increasing when the Reynolds number is changing from 32,000 to 95,000. The reason is that when the fluid flows through the orifice plate, the flow field will change considerably, and the inclination angle is favorable for the development and stabilization of the flow field. At this point, the larger of the inclination angle is the more favorable for the development and stabilization of the flow field. When the gas flow rate range is 5–15 m/s, and the inclination angle of the orifice flowmeter are set as 40°, 45° and 60°, the AARE of discharge coefficient are 1.11%, 0.77% and 0.54%, respectively. Therefore, the measurement accuracy is the highest when bevel angle of the ICOF is 60° at 5–15 m/s.

6. Conclusions

To overcome the shortcomings of low hardness and poor wear resistance of the TSSOF, an improved carbide orifice flowmeter was manufactured by placing the cemented carbide in the round hole of the TSSOF. Through field experiment, the change in the entrance sharpness for the two types of orifice flowmeters were compared; the FLUENT software was used to establish the simulation model, and the discharge coefficient which was used to characterize the measurement accuracy of the flowmeter was calculated, then it was compared with the result calculated by the ISO empirical correlation; additionally, the influence of the downstream inclination angle of the orifice plate on the measurement accuracy was studied. Thus, the following conclusions can be drawn:

- (1) Through the field experiment, it is concluded that the entrance sharpness of the two kinds of orifice flowmeters was increased with the increasing of use time, but the change rate of the ICOF is smaller. Therefore, the ICOF has a better performance in wear resistant property, and its measurement accuracy is also higher.
- (2) Based on the established simulation model, the discharge coefficient values of the two types of orifice flowmeters were calculated and compared with the computed values of the ISO correlation. The accuracy of the ICOF measurement accuracy is higher than that of the TSSOF. At the same detection time and the gas flow rate range of 5–15 m/s, the maximum value of AARE for the ICOF is 2.12%, while the maximum value of AARE for the TSSOF reached 4.10%; the AARE of the ICOF can be increased to 1.98%, and its measurement accuracy can be achieved up to 2.39 times of the TSSOF.

- (3) In the case of gas flow rates are 5 m/s, 8 m/s, 10 m/s, 12 m/s and 15 m/s, the AARE of the ICOF will not exceed 2%, while the AARE of the TSSOF reached 3.95%; at the same gas flow rate, the AARE of the ICOF can be reach to 2.07%, the measurement accuracy can be up to 2.20 times of the TSSOF; in addition, the standard deviation of the AARE for the ICOF is less than that of the TSSOF, therefore, the ICOF measurement accuracy is more stable and reliable.
- (4) Through researching bevel angle, it is found that when the natural gas flow rate range is 5–15 m/s and the downstream inclination angle is 60°, the measurement accuracy of the ICOF is the highest. Therefore, the ICOF with high strength and high wear resistance is more suitable for engineering practice.

Acknowledgements

This work was supported by the National Natural Science Foundation of China under grant number 51474184 and the subproject of the National Science and Technology Major Project of China under grant number 2011ZX05054.

References

- [1] R.W. Miller, *Flow measurement engineering handbook*, (1983).
- [2] G.L. Morrison, K.R. Hall, J.C. Holste, M.L. Macek, L.M. Ihfe, R.E. DeOtte Jr., D.P. Terracina, Comparison of orifice and slotted plate flowmeters, *Flow. Meas. Instrum.* 5 (2) (1994) 71–77.
- [3] L. Shenmin, Calculation method of gas flow measurement with ynz inner-cone flowmeter, *Nat. Gas. Ind.* 10 (2004) 039.
- [4] T. Jin, H. Tian, X. Gao, Y. Liu, J. Wang, H. Chen, Y. Lan, Simulation and performance analysis of the perforated plate flowmeter for liquid hydrogen, *Int. J. Hydrog. Energy* 42 (6) (2017) 3890–3898.
- [5] M. Reader-Harris, N. Barton, D. Hodges, The effect of contaminated orifice plates on the discharge coefficient, *Flow. Meas. Instrum.* 25 (2012) 2–7.
- [6] K. Doblhoff-Dier, K. Kudlaty, M. Wiesinger, M. Gröschl, Time resolved measurement of pulsating flow using orifice, *Flow. Meas. Instrum.* 22 (2011) 97–103.
- [7] A. Svete, J. Kutin, I. Bajsic, J. Slavic, Development of a liquid-flow pulsator, *Flow. Meas. Instrum.* 23 (2012) 1–8.
- [8] A. Erdal, H. Andersson, Numerical aspects of flow computation through orifices, *Flow. Meas. Instrum.* 8 (1) (1997) 27–37.
- [9] C.L. Hollingshead, M.C. Johnson, S.L. Barfuss, R.E. Spall, Discharge coefficient performance of Venturi, standard concentric orifice plate, V-cone and wedge flow meters at low Reynolds numbers, *J. Pet. Sci. Eng.* 78 (3) (2011) 559–566.
- [10] M.S. Shah, J.B. Joshi, A.S. Kalsi, C.S.R. Prasad, D.S. Shukla, Analysis of flow through an orifice meter: cfd simulation, *Chem. Eng. Sci.* 71 (2012) 300–309.
- [11] D. He, B. Bai, J. Zhang, X. Wang, Online measurement of gas and liquid flow rate in wet gas through one V-Cone throttle device, *Exp. Therm. Fluid Sci.* 75 (2016) 129–136.
- [12] S.N. Singh, V. Seshadri, R.K. Singh, R. Gawhade, Effect of upstream flow disturbances on the performance characteristics of a V-cone flowmeter, *Flow. Meas. Instrum.* 17 (5) (2006) 291–297.
- [13] A. McIver, R.J.W. Peter, The use of a V-cone fuel flow meter to measure the coke oven gas and natural gas flow in a combined heat and power plant, In *IDEA Proceedings of the 95th Annual Conference Trade Show*, Seattle Washington, 2004.
- [14] Y. Geng, J. Zheng, T. Shi, Study on the metering characteristics of a slotted orifice for wet gas flow, *Flow. Meas. Instrum.* 17 (2) (2006) 123–128.
- [15] G. Annamalai, S. Pirouzpanah, S.R. Gudigopuram, G.L. Morrison, Characterization of flow homogeneity downstream of a slotted orifice plate in a two-phase flow using electrical resistance tomography, *Flow. Meas. Instrum.* 50 (2016) 209–215.
- [16] S. Pirouzpanah, M. Cevik, G.L. Morrison, Multiphase flow measurements using coupled slotted orifice plate and swirl flow meter, *Flow. Meas. Instrum.* 40 (2014) 157–161.
- [17] C. Hua, Y. Geng, Wet gas metering technique based on slotted orifice and swirl-meter in series, *Flow. Meas. Instrum.* 30 (2013) 138–143.
- [18] B.B. Manshoor, F. Nicolleau, S. Beck, The fractal flow conditioner for orifice plate flow meters, *Flow. Meas. Instrum.* 22 (3) (2011) 208–214.
- [19] S. Malavasi, G. Messa, U. Fratino, A. Pagano, On the pressure losses through perforated plates, *Flow. Meas. Instrum.* 28 (2012) 57–66.
- [20] T. Ma, D. Wang, B. Zhang, Z. Lin, Experimental on metering characteristics of multi-hole orifice, *Nucl. Power Eng.* 31 (2) (2010) 126–130.
- [21] S. Huang, T. Ma, D. Wang, Z. Lin, Study on discharge coefficient of perforated orifices as a new kind of flowmeter, *Exp. Therm. Fluid Sci.* 46 (2013) 74–83.
- [22] V. Singh, T.J. Tharakan, Numerical simulations for multi-hole orifice flow meter, *Flow. Meas. Instrum.* 45 (2015) 375–383.
- [23] E. Schena, S. Cecchini, S. Silvestri, An orifice meter for bidirectional air flow measurements: influence of gas thermo-hygrometric content on static response and bidirectionality, *Flow. Meas. Instrum.* 34 (2013) 105–112.
- [24] A.L. Song, G.C. Liang, Analysis of the measurement accuracy of differential pressure orifice flowmeter, *Drill. Prod. Technol.* 29 (2) (2006) 114–115.
- [25] A. Abou El-Azm Aly, A. Chong, F. Nicolleau, S. Beck, Experimental study of the